Electron–ion recombination in strongly coupled cold plasmas under nonequilibrium conditions

2006 J. Phys. A: Math. Gen. 39 4571

(http://iopscience.iop.org/0305-4470/39/17/S41)

INSTITUTE OF PHYSICS PUBLISHING JOURNAL OF PHYSICS A: MATHEMATICAL AND GENERAL

J. Phys. A: Math. Gen. **39** (2006) 4571–4577 doi:10.1088/0305-4470/39/17/S41

Electron–ion recombination in strongly coupled cold plasmas under nonequilibrium conditions

T Pohl[1] **and T Pattard**

Max Planck Institute for the Physics of Complex Systems, Nöthnitzer Str 38, D-01187 Dresden, Germany

Received 30 September 2005, in final form 11 December 2005
Published 7 April 2006
Online at stacks.iop.org/JPhysA/39/4571

Abstract

We discuss the dynamics of recombination of an expanding ultracold plasma into highly excited Rydberg states, with emphasis on the influence of possible strong coupling between the charges and the nonequilibrium character of the electronic component. While the former does not significantly affect recombination in current experimental scenarios, the latter is shown to have a considerable influence on the system dynamics. We derive correction factors quantifying the deviation of collision rates from their respective equilibrium values. The experimentally observed unexpectedly high recombination rate at long evolution times can be reproduced by a proper inclusion of these effects without the need to invoke alternative, previously suggested mechanisms, such as an 'adiabatic motional recombination' or the development of very strong electron correlations by collisional cooling.

PACS numbers: 52.20.−j, 52.25.Dg

1. Introduction

Since their first experimental realization in 1999, ultracold ($T \ll 1$ K) quasineutral plasmas [1] have gained an increasing amount of attention both from experimentalists and theoreticians [2–10]. The appeal of these systems is based on essentially two remarkable properties. First, the ultralow temperatures of the plasma suggest that the system might be in a very strongly coupled regime otherwise realized mostly in exotic astrophysical objects. While early hopes of observing Coulomb crystallization in such a plasma have not materialized yet due to various intrinsic heating mechanisms, moderately strong coupling is still observed and significantly affects the system evolution. Moreover, from the way the plasma is created by photoionization of a cloud of neutral atoms, the system is in a state far from thermodynamical equilibrium. On the one hand, the spatial distribution of the ions is fully uncorrelated initially. On the

[1] Present address: ITAMP, Harvard-Smithsonian Center for Astrophysics, 60 Garden Street, Cambridge, MA 02138, USA.

other hand, the velocity distribution of the electrons is given by a microcanonical rather than a thermal distribution immediately after the photoionization. Furthermore, the finite depth of the potential generated by the ionic space charge implies deviations from a Maxwell–Boltzmann distribution even at later times. Experimentally, the huge amount of control possible with state-of-the-art techniques makes a very precise preparation of initial states possible. Moreover, convenient timescales allow for detailed measurements of the time evolution of the plasma, making ultracold plasmas an almost ideal system for experimental studies of strongly coupled nonequilibrium systems.

Meanwhile, theoretical approaches have been developed for the description of various aspects of the dynamics of ultracold plasmas which are in very good agreement with experimental observations [8, 11]. The time evolution of macroscopic properties, such as temperatures, densities, expansion velocities, etc, can be described even with simple hydrodynamical approaches [12, 13], while ionic correlation effects can accurately be treated using a hybrid molecular dynamics method [13]. So far, the dynamics of bound-state formation through electron–ion recombination has withstood a quantitative modelling (see [14]). Firstly, the timescale of the initial population of bound states is not accurately reproduced by the current numerical simulations. Moreover, the rate of recombination at long times observed experimentally is larger than that predicted by existing theories. While there have been attempts to explain the observed behaviour by proposing new recombination mechanisms such as 'adiabatic motional recombination' caused by a time-dependent continuum shift [15] or the development of strong electron correlations by collisional cooling [16], these explanations remain controversial. Since the former approach neglects the initial correlation-induced heating and electronic field effects on continuum lowering, the respective continuum shift is overestimated by an order of magnitude resulting in an overestimate of the corresponding 'motional recombination' rate. On the other hand, the results of [16] are inconsistent with recent temperature measurements [3, 4], proving the existence of well-separated temperatures for the electronic and ionic subsystems. This discrepancy is mainly due to overestimated electron–ion collision rates used in [16].

In the present paper, we analyse the role of strong coupling as well as nonequilibrium effects on the recombination behaviour. As it turns out, properly accounting for these effects within existing theoretical approaches leads to reasonable agreement with experimental observations without the need of invoking new recombination mechanisms.

2. Basic model

Despite their very low temperatures, typical densities of ultracold plasmas are sufficiently low that the corresponding Fermi temperature is well below the electron temperature and quantum statistical effects can safely be neglected. Hence, classical molecular dynamics simulations are expected to provide a very accurate description of these plasmas. Indeed, it has been demonstrated that they permit an accurate study of recombination on a short timescale [7, 9]. On the other hand, the huge particle numbers required and the extreme separation of the electronic and ionic timescales make them unsuitable for investigations of the long-time plasma dynamics, rendering a direct comparison with present experiments practically impossible.

One approach to overcome this problem in the framework of a hydrodynamical model has been described in detail in [13]. Briefly, we start from the classical kinetic equations of the electronic and ionic subsystems, respectively, which together with the assumption of quasineutrality and a local density approximation for the ionic correlation function allows us to derive a closed set of ordinary differential equations for the width of the plasma cloud, the expansion velocity, and electronic and ionic temperatures. In order to take into account

inelastic processes, these equations are coupled to a set of rate equations describing the population dynamics of formed atoms. We account for radiative processes such as spontaneous decay to lower levels and radiative recombination [12, 17] as well as collision processes such as electron-impact (de)excitation, electron-impact ionization and three-body recombination. The latter are described by the classical collision rates given in [18].

3. Strong coupling effects

Since the bound electrons typically occupy very highly excited Rydberg states, the collision rates obtained in [18] from classical trajectory Monte Carlo calculations are expected to yield reliable results for collisions taking place in vacuum. However, for these highly excited states level shifts caused by correlations between the charges may lead to a significant modification of the collision rates even at the extremely low densities realized in ultracold plasmas. In the simplest approximation, the level shift may be assumed to be independent of the respective binding energy, leading to the well-known Stewart–Pyatt expression [19]

$$\Delta E = \frac{e^2}{a}[2(\Gamma_e + \Gamma_i)]^{-1}[(1 + 3^{3/2}(\Gamma_e + \Gamma_i)^{3/2})^{2/3} - 1], \tag{1}$$

valid for two-temperature plasmas in individual equilibrium, where Γ_e and Γ_i are the Coulomb coupling parameters of electronic and ionic subsystems, respectively[2]. Since the timescale of the electronic dynamics, of the order of some ns, is the shortest timescale in the system, this is certainly a good approximation for the electronic subsystem. On the other hand, the build-up of ionic correlations proceeds on a much slower timescale of μs. However, the static level shift is uniquely determined by the corresponding spatial correlation function of the ions, while locally large fields due to the presence of nearby electrons or ions average out in a neutral plasma. As we have shown previously [10], the spatial ion correlation function resembles the equilibrium form but parametrized by an effective Coulomb coupling parameter, even at the early stages of the plasma evolution. Hence, we use this effective ionic coupling parameter to determine the time-dependent level shift from equation (1).

In the simplest approximation, the recombination rate is only weakly affected by the nonideality of the plasma, while the ionization rate is enhanced by a factor of roughly $\exp(\Delta E/k_B T_e)$ at small electron coupling (see e.g. [20]). As discussed in [21], this static screening correction yields a good description of ionization processes, in particular since the smallest atomic binding energies, given by $k_B T_e$, are much larger than the energy of electronic plasma oscillations which are of the order of 10 mK for the highest densities of 10^9 cm^{-3}. Although strong-coupling corrections to the individual recombination rates are weak and hence not considered here, the level shift (1) may decrease the total rate of recombination by setting an upper limit for bound levels $n_{stat} = \sqrt{\mathcal{R}/\Delta E}$ in addition to the Thomson value of $n_{therm} = \sqrt{\mathcal{R}/k_B T_e}$, where $\mathcal{R} = 13.6$ eV denotes the Rydberg energy. This fact has also been discussed in [15] as possibly important in ultracold plasmas. However, the influence of electronic electrostatic fields as well as the initial correlation-induced heating of the ions has been neglected there, resulting in an overestimate of the level shift by an order of magnitude and therefore in a much too low recombination rate. For the plasma parameters realized in the experiment [2], the strong-coupling corrections discussed above do not lead to qualitative changes of the recombination dynamics, but are expected to be important for the short-time

[2] In the present situation of an inhomogeneous plasma with a Gaussian density profile, we define the respective Coulomb coupling parameter as $\Gamma_{e/i} = e^2/(k_B T_{e/i} a)$, where $a = (4\pi\bar{\rho}/3)^{-1/3}$, $\bar{\rho} = N_i/(4\pi\sigma^2)^{3/2}$ is the average ion density and σ is the width of the plasma cloud.

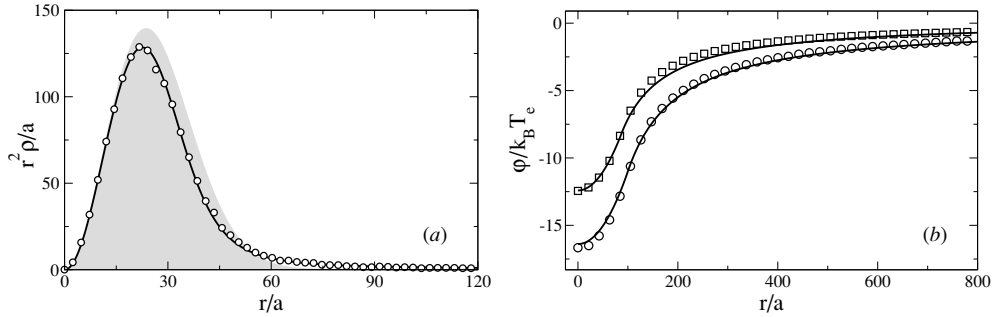

Figure 1. (*a*) Comparison of the electron density obtained from a full MD simulation (circles) of 50 000 ions and electrons with $\Gamma_e\ (t = 0) = 0.5$ with the corresponding Michie–King distribution (solid line). The shaded area shows the ion density profile. (*b*) Numerically calculated electrostatic potential for $N_i = 300\,000$, $\Gamma_e = 0.2$ (circles) and $N_i = 300\,000$, $\Gamma_e = 0.05$ (squares), compared to the fit formula equation (4).

dynamics at still lower electron temperatures and for alternative scenarios as considered, e.g., in [22].

4. Nonequilibrium effects

Another modification of the collision rates results from deviations from the commonly assumed Maxwellian distribution of electron velocities, which does not hold for finite-size plasmas. Since there is no external trapping potential, electrons evaporate from the plasma until the resulting charge imbalance becomes large enough to trap the remaining electrons, which quickly reach a quasi-steady state forming a temporarily quasineutral plasma in the central region of the cloud. As first discussed in connection with studies of globular star clusters, the resulting steady state is well represented by a truncated Maxwell–Boltzmann distribution [13, 24]

$$f_e(\mathbf{r},\mathbf{v}) \propto \exp\left(-\frac{\varphi(r)}{k_B T_e}\right) \begin{cases} \exp\left(-\dfrac{m_e v^2}{2k_B T_e}\right) - \exp\left(-\dfrac{m_e v_c^2}{2k_B T_e}\right), & v \leqslant v_c, \\ 0, & v > v_c, \end{cases} \tag{2}$$

where the space charge potential φ has to be determined from $\Delta\varphi = 4\pi e^2(\rho_e - \rho_i)$ and $v_c = \sqrt{2\varphi/m_e}$ denotes the escape velocity[3]. In order to demonstrate the quality of this expression, we compare in figure 1(*a*) the resulting density profile, the so-called Michie–King distribution, with the electron density obtained from a full molecular dynamics simulation for a relatively large particle number of 10^5.

Consequently, the correct collision rates have to be obtained by using the steady-state distribution equation (2) instead of a Maxwellian, leading to a correction factor

$$\kappa(r) = \frac{\int_0^{\varphi} \sqrt{E}\sigma(E) f_{MK}(E)\,\mathrm{d}E}{\int_0^{\varphi} f_{MK}(E)\,\mathrm{d}E} \frac{\int_0^{\infty} f_{MB}(E)\,\mathrm{d}E}{\int_0^{\infty} \sqrt{E}\sigma(E) f_{MB}(E)\,\mathrm{d}E}, \tag{3}$$

where $f_{MB} \propto \sqrt{E}\exp(-E/k_B T_e)$ denotes the Maxwell–Boltzmann distribution and $f_{MK} \propto \sqrt{E}(\exp(-E/k_B T_e) - \exp(-\varphi/k_B T_e))$. The required collision cross sections $\sigma(E)$ are obtained from an inverse Laplace transform of the original rates. This procedure leads to

[3] Note that this relation implies a monotonic space dependence of φ. The general case has been discussed in [13].

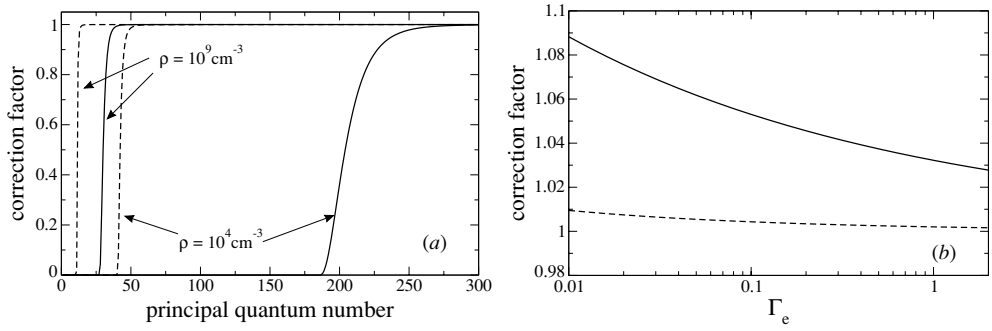

Figure 2. (*a*) Average correction factor $\bar{\kappa}$ for ionization rates (solid line) and $n \to n+1$ excitation rates (dashed line) for $N_i = 500\,000$ and $\Gamma_e = 0.2$ at two different densities, as indicated by the arrows. (*b*) Average correction factor for recombination rates (solid line) and total deexcitation rates (dashed line) for $N_i = 500\,000$.

an additional space dependence of the collision rates via the potential $\varphi(r)$. Finally, an average correction coefficient $\bar{\kappa}$ may be calculated by integrating over the Gaussian density profile. The resulting correction factor only depends on the ion number N_i, the electronic Coulomb coupling parameter Γ_e and the transition energy in units of e^2/a, $\varepsilon = E\big/(e^2/a)$.

In order to simulate the plasma evolution including these corrections, we have numerically calculated the required space charge potential for a broad range of parameters, two examples of which are shown in figure 1(*b*). Note that φ can be well fitted by the potential of a homogeneously charged sphere

$$\varphi \approx F_0 R^3 \begin{cases} r^2/(2R^3) - 3/(2R), & r \leqslant R, \\ -1/r, & r > R, \end{cases} \tag{4}$$

with $R = 0.73 N_i^{0.404} \Gamma_e^{0.105}$ and $F_0 = k_B T_e a^2/\sigma^2 = (e^2/a)(6\sqrt{\pi}/N_i)^{2/3}\Gamma_e^{-1}$, an observation which might prove to be very useful for future temperature measurements as described in [4, 22].

In figure 2, we show the parameter dependence of the rate corrections $\bar{\kappa}$ for (de)excitation, ionization as well as recombination. While the corrections for the recombination and deexcitation rates do not depend on the associated transition energy and these rates are only slightly enhanced, the ionization and excitation rates quickly drop to zero below a critical quantum number n_c. This sudden decrease takes place when the potential depth $-\varphi(0)$ becomes smaller than the corresponding transition energy, since there is no electron left in the plasma which could drive this transition. As we show below, this effect may lead to considerable changes of the recombination dynamics due to the drastic decrease of the potential depth during the plasma expansion.

5. Results and discussion

Before comparing our results with the measurements [2], some details of this experiment need to be discussed. Experimentally, the number of Rydberg atoms has been determined by analysing the signal obtained by applying an electrical field ramp to the plasma. In order to avoid any further electron–atom collisions during this field ramp, an additional 10 μs field pulse was used prior to the Rydberg atom detection to strip away free plasma electrons. We have therefore shifted the experimental curve by -10 μs. Furthermore, only a finite window $n_l < n < n_u$ of Rydberg levels could be detected in the experiment since more deeply bound

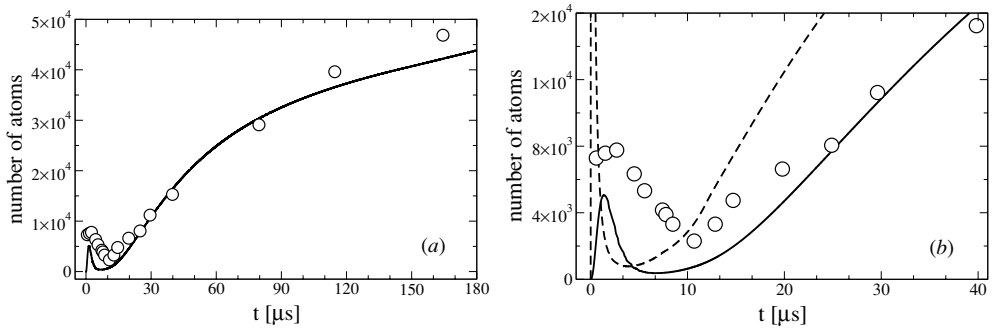

Figure 3. Comparison of the calculated (solid line) time dependence of the number of Rydberg atoms with the experiment [2] (circles) for $N_i\ (t=0) = 700\,000$, $\rho\ (t=0) = 2.7\times10^9\ \mathrm{cm}^{-3}$ and $T_e\ (t=0) = 6$ K. The dashed line in (*b*) shows the result without the effect of ionic microfields (see the text). Since there is an experimental uncertainty of a factor of 2 in the number of Rydberg atoms due to detector calibration [2], we have scaled down the experimental curve by a factor of 1.6.

states $n < n_l$ were not ionized by the field ramp while more weakly bound states $n > n_u$ were already destroyed by the stripping field. From the respective maximum field strengths F of the pre-ionization pulse and the detection ramp, and by using the relation [2]

$$F_n = \frac{\tilde{F}}{6n^4}, \qquad \tilde{F} = 5.14\times10^9\ \mathrm{V\,cm^{-1}}, \tag{5}$$

this window has been determined to be $40 \leqslant n \leqslant 100$. However, after removing the free electrons, the plasma becomes strongly charged, resulting in strong electric microfields which may change the above window of detectable Rydberg levels. Measurements of such microfields [23] reveal that they are indeed strong enough to significantly disturb the observed field-ionization spectrum. As a simple estimate of this effect, we add the average electric field, as calculated in [23], to the field-ionization ramp, from which we obtain a time-dependent window of detectable Rydberg atoms by using equation (5).

A comparison between the experimental atom number dynamics[4] and the present calculation including strong-coupling effects, nonequilibrium effects and the influence of ionic microfields is shown in figure 3. As can be seen, there is reasonable agreement for the long-time evolution of the Rydberg atom number as well as for the short-time behaviour. As discussed in [12], the nonmonotonic atom number evolution is entirely due to the finite window of detectable Rydberg states. In fact, the total number of atoms is found to increase monotonically, in contrast to the conclusions reached in [16]. On the other hand, the result without taking into account the level shift by ionic microfields yields a far too large initial atom number and a too short timescale for the initial rise. The improved agreement, even with our simple estimate of the resulting level shifts, reveals the importance of electrical microfields in interpreting field-ionization spectra.

At long times, the number of Rydberg atoms grows stronger than what has been predicted using the rates from [18]. This can be attributed to the fact that the density, and hence the depth of the ionic potential well φ, significantly decreases during the plasma expansion. As a consequence, the critical quantum number n_c below which the ionization rate drops to zero (figure 2(*a*)) increases continuously, shifting the balance between recombination of

[4] Since there is an experimental uncertainty of a factor of 2 in the number of Rydberg atoms due to detector calibration [2], we have scaled down the experimental curve by a factor of 1.6.

free electrons and re-ionization of bound states. Taking this effect into account leads to a reasonable agreement with the experimental results even for the later stages of the plasma evolution.

In conclusion, incorporating strong-coupling effects as well as the influence of the nonequilibrium electronic velocity distribution on the recombination behaviour of ultracold quasineutral plasmas leads to results in reasonable agreement with experimental measurements. This seems to obliviate the need for invoking alternative, more exotic recombination mechanisms.

Acknowledgment

We would like to thank Jan-Michael Rost for many helpful discussions.

References

[1] Killian T C, Kulin S, Bergeson S D, Orozco L A, Orzel C and Rolston S L 1999 *Phys. Rev. Lett.* **83** 4776
[2] Killian T C, Lim M J, Kulin S, Dumke R, Bergeson S D and Rolston S L 2001 *Phys. Rev. Lett.* **86** 3759
[3] Chen Y C, Simien C E, Laha S, Gupta P, Martinez Y N, Mickelson P G, Nagel S B and Killian T C 2004 *Phys. Rev. Lett.* **93** 265003
[4] Roberts J L, Fertig C D, Lim M J and Rolston S L 2004 *Phys. Rev. Lett.* **92** 253003
[5] Cummings E A, Daily J E, Durfee D S and Bergeson S D 2005 *Preprint* physics/0506069
[6] Murillo M S 2001 *Phys. Rev. Lett.* **87** 115003
[7] Mazevet S, Collins L A and Kress J D 2002 *Phys. Rev. Lett.* **88** 055001
[8] Robicheaux F and Hanson J D 2002 *Phys. Rev. Lett.* **88** 055002
[9] Kuzmin S G and O'Neil T M 2002 *Phys. Rev. Lett.* **88** 065003
[10] Pohl T, Pattard T and Rost J M 2005 *Phys. Rev. Lett.* **94** 205003
[11] Pohl T and Pattard T 2005 *J. Phys.: Conf. Ser.* **11** 223
[12] Robicheaux F and Hanson J D 2003 *Phys. Plasmas* **10** 2217
[13] Pohl T, Pattard T and Rost J M 2004 *Phys. Rev.* A **70** 033416
[14] Rolston S L and Roberts J L 2002 *XVIII ICAP 2002 Proceedings* (online: http://cfa-www.harvard.edu/~hrs/icap2-2/proceedings/Rolston.pdf)
[15] Hahn Y 2001 *Phys. Rev.* E **64** 046409
[16] Zelener B B, Zelener B V and Manykin E A 2004 *JETP* **99** 1173
[17] Stevefelt J, Boulmer J and Delpech J F 1975 *Phys. Rev.* A **12** 1246
[18] Mansbach P and Keck J 1969 *Phys. Rev.* **181** 275
[19] Stewart J C and Pyatt K D Jr 1966 *Astrophys. J.* **144** 1203
[20] Schlanges M, Bornath T and Kremp D 1988 *Phys. Rev.* A **38** 2174
[21] Murillo M S and Weisheit J C 1998 *Phys. Rep.* **302** 1
[22] Vanhaecke N, Comparat D, Tate D A and Pillet P 2005 *Phys. Rev.* A **71** 013416
[23] Feldbaum D, Morrow N V, Dutta S K and Raithel G 2002 *Phys. Rev. Lett.* **89** 173004
[24] Comparat D, Vogt T, Zahzam N, Mudrich M and Pillet P 2005 *Mon. Not. R. Astron. Soc.* **361** 1227